The *FA2* gene of *Chlamydomonas* encodes a NIMA family kinase with roles in cell cycle progression and microtubule severing during deflagellation

Moe R. Mahjoub, Ben Montpetit, Lifan Zhao, Rip J. Finst, Benjamin Goh, Apollos C. Kim and Lynne M. Quarmby*

Department of Biological Sciences, Simon Fraser University, 8888 University Drive, Burnaby, BC, Canada V5A 1S6

*Author for correspondence (e-mail: Quarmby@sfu.ca)

Accepted 13 January 2002

Journal of Cell Science 115, 1759-1768 (2002) © The Company of Biologists Ltd

Summary

The NIMA kinases are one of several families of kinases that participate in driving the eukaryotic cell cycle. NIMA-related kinases have been implicated in G2/M progression, chromatin condensation and regulation of the centrosome cycle. Here we report the identification of a new member of this family, *FA2*, from *Chlamydomonas reinhardtii*. *FA2* was originally discovered in a genetic screen for deflagellation-defective mutants. We have previously shown that *FA2* is essential for basal-body/centriole-associated microtubule severing. We now report that the *FA2* NIMA-related kinase also plays a role in cell cycle progression in *Chlamydomonas*. This is the first indication that members of the NIMA family might exert their effects through the regulation of microtubule severing.

Key words: NIMA, Cell cycle, *Chlamydomonas*, Microtubule severing, Deflagellation

Introduction

Protein phosphorylation is central in the regulation of eukaryotic cell cycle progression. Among the several families of kinases that contribute to cell cycle control are the NIMA kinases. The founding member of the NIMA family is a serine/threonine kinase that plays an essential role in regulating the G2/M transition in *Aspergillus nidulans* (NIMA; never in mitosis) (Lu and Means, 1994; Morris, 1976; Osmani et al., 1991). The *Aspergillus* NIMA protein also promotes chromosome condensation (O'Connell et al., 1994; Osmani et al., 1988) and plays a role in the localization of cyclin B to the nucleus in late G2 (Wu et al., 1998). Studies of NIMA-related kinases (Neks) suggest that this family of proteins may serve diverse cellular functions. For example, mammalian Nek6 and Nek7 appear to mediate activation of the p70 ribosomal S6 kinase in response to insulin and growth factor stimulation (Belham et al., 2001), whereas a Nek1 mouse knock-out has a pleiotropic phenotype, including a progressive polycystic kidney disease (Upadhya et al., 2000). Whether the protein synthesis activities of Neks 6 and 7 or the PKD phenotype of the *Nek1* mutant mouse ultimately relate to cell cycle control remains to be determined. Nevertheless, other members of the family are clearly involved in the regulation of cell cycle progression.

Nek2 is of particular interest with respect to the present work. Expression studies have implicated vertebrate Nek2 in cell cycle progression, but there is no evidence that it is playing the same roles as NIMA in G2/M transition and chromosome condensation (Fry et al., 1995; Fry et al., 1998; Rhee and Wolgemuth, 1997; Tanaka et al., 1997). Instead, Nek2 appears to play an essential role in the progression of the centrosomal cycle. Overexpression of Nek2 results in premature separation of the replicated centrioles (Fry et al., 1998; Mayor et al., 2000). Furthermore, biochemical data demonstrates that Nek2B facilitates assembly of the *Xenopus* zygotic centrosome (Fry et al., 2000). Like Nek2, the *FA2* gene of *Chlamydomonas* encodes a NIMA family kinase that has a centrosome/basal-body-associated function.

The *FA2* gene was discovered during a genetic screen for deflagellation-defective mutants of *Chlamydomonas reinhardtii* (Finst et al., 1998). Deflagellation is a highly specific process that involves a Ca^{2+} signal transduction pathway originating at the plasma membrane and culminating in the severing of the nine outer-doublet axonemal microtubules at a precise site distal to the transition zone between the axoneme and the basal bodies (for a review, see Quarmby, 2000). The microtubule-severing ATPase katanin has been implicated in this severing event by its localization at the site of severing, the inhibition of calcium-induced severing by katanin p60 antibodies and its demonstrated ability to sever the complex doublet microtubules of the axoneme (Lohret et al., 1998). Our genetic screen identified three additional genes, *ADF1*, *FA1* and *FA2*, which are essential for in vivo deflagellation. *ADF1* plays a role in signal transduction, whereas, cells with mutations in either *FA1* or *FA2* fail to deflagellate because of a defect in calcium-induced axonemal microtubule severing (Finst et al., 1998; Quarmby, 1996). Fa1p is a novel 170 kDa protein with a large coiled coil domain; it localizes to the base of the flagella (Finst et al., 2000).

In this work we have identified a genomic clone that rescues *fa2* mutants. Sequence analysis indicates that the *FA2* gene encodes a NIMA kinase. This is the first indication that this

family of kinases might play a role in the regulation of microtubule severing. It is clear that microtubules break in vivo (e.g. Odde et al., 1999), and regulated microtubule severing probably plays a role in the establishment of non-centrosomal microtubules in neurons, myocytes and epithelial cells (Ahmad et al., 1999; Rodionov et al., 1999; Waterman-Storer and Salmon, 1997; Odde et al., 1999). Furthermore, immunolocalization, genetic and biochemical evidence suggest that katanin is important in mitotic and meiotic cell division (McNally et al., 1996; McNally and Thomas, 1998; McNally et al., 2000; Srayko et al., 2000). The role(s) of microtubule severing during the cell cycle, and the regulation of microtubule severing in general remain unclear. Whether Fa2p regulates centrosome-associated microtubule severing or, like Nek2, plays a role in centrosome assembly (or both), it was of interest to discover in the current work that *fa2* mutants are delayed in cell cycle progression.

Materials and Methods

Cell strains and culture

Chlamydomonas strains B214 (obtained from G. Pazour, University of Massachusetts) and strain cc620 (obtained from the *Chlamydomonas* Genetics Center, Durham, NC) were used as the wild-type strains. Mutant strains *fa2-1*, *fa2-2*, *fa2-3* and *fa2-4* were isolated in our laboratory as previously described (Finst et al., 1998). Cells were maintained in liquid TAP medium or on plates (1.5% agar) (Harris, 1989) at 22°C with constant illumination. Nit1$^+$ transformants (see below) were selected by growth on SGII(NO_3) media (Sager and Granick, 1953; Fernandez et al., 1989). All *arg7* strains were maintained on medium supplemented with 0.02% arginine (Sigma, St Louis, MO) or on media supplemented with 4 g/*l* yeast extract. All *ble* transformants were grown on 1.5% TAP plates supplemented with Zeocin (40 μg/ml; Invitrogen, Carlsbad, CA).

Genomic library and BAC DNA screening

An insertion of exogenous *NIT1* DNA (in pUC119 plasmid) genetically mapped to the *FA2* locus in the *fa2-3* strain (Finst et al., 1998) and was therefore used as a molecular tag to clone flanking DNA. A lambda Fix II bacteriophage library of *fa2*-3 was created according to manufacturers instructions (Stratagene, La Jolla, CA). The library was screened with radiolabelled fragments of the transforming DNA (specifically, pUC119 and 0.9 kb of the 3′ end of *NIT1*) as described by Finst and coworkers (Finst et al., 2000). Following identification of positive clones, a 1.5 kb fragment flanking the inserted DNA was used to probe a wild-type *Chlamydomonas* genomic BAC library (Incyte Genomics, St. Louis, MO). To verify specificity of cross-reactivity, DNA of positive BAC clones was isolated (as described by Incyte Genomics) and hybridized on Southern blots with the same 1.5 kb fragment described above.

Mutant rescue, *FA2* genomic and cDNA isolation

To determine whether positive BAC clones could rescue the deflagellation defect of *fa2* mutants, *fa2-2* cells (*nit*–) were co-transformed with *NIT1* and BAC DNA. Nit1$^+$ transformants were selected and assayed for deflagellation as previously described (Finst et al., 1998). A BAC clone that rescued the deflagellation defect in *fa2-2* mutants was digested with various endonucleases including *Eco*RI, *Sal*I, *Sac*I, *BamH*I, *Pst*I and *Apa*I. The products of these digests were co-transformed with *NIT1* into *fa2-2* cells to identify enzymes whose recognition sites did not fall within the *FA2* gene. As reported below, one subclone, containing a 4.6 kb *Sac*I-*Sal*I insert, rescued the deflagellation defect. To confirm that the 4.6 kb fragment was responsible for the rescue, it was co-transformed with another selectable marker pARG7.8 (encoding arginosuccinate lyase, linearized by digestion with *Bam*HI) (Debuchy et al., 1989) into *fa2-1 /arg7*– cells. Arg7$^+$ transformants were selected by growth on medium lacking arginine and assayed for deflagellation. The 4.6 kb subclone was sequenced by the Emory University DNA Sequence Facility (Atlanta, GA) and the University of British Columbia DNA Sequencing Laboratory (Vancouver, BC, Canada).

In order to identify the cDNA, RNA isolation and RT-PCR were performed as previously described (Finst et al., 2000). Polyadenylated RNA was isolated from wild-type strain cells (strain B214) and reverse transcribed using Superscript II reverse transcriptase (Life Technologies, Gaithersburg, MD) and oligo(dT)$_{(12\text{-}18)}$ primers. The PCR primers were designed according to putative exon sequences predicted by the GeneMark algorithm (Benian et al., 1996). 3′ RACE was then performed as previously described (Finst et al., 2000). PCR products were separated by agarose gel electrophoresis, purified using an ultra-MC filter unit (Millipore, Bedford MA) and subcloned into the pGEMT-Easy vector (Promega, Madison, WI) prior to sequencing.

Sequence analysis

Searches of the GenBank database were performed using the BLAST program (Altschul et al., 1997). The top hits from the BLAST search were aligned with the amino-acid sequence of *FA2* using Clustal W (Thompson et al., 1994) and Genedoc (Nicholas et al., 1997). The catalytic kinase domain and ATP-binding site were identified by eye using consensus sequences (Hayashi et al., 1999). Phylogenetic analysis was performed using the PHYLIP package (Felsenstein, 1989) and PhyloBLAST (Brinkman et al., 2001).

FA2 RNAi construct

The goal for the FA2 RNAi construct was to produce a transgene which, when transcribed by *Chlamydomonas*, would produce a double-stranded RNA structure. In order to achieve efficient expression, we started with the 5′ end of the genomic clone, containing upstream sequence and introns presumed to be important for efficient expression. Specifically, the *FA2* genomic clone was digested with *NruI* (3108) and *SalI* (4657) in order to release the 3′ end of the gene (a fragment of about 1.5 kb from the middle of exon 5 through to the end of the genomic clone). Similarly, the *FA2* cDNA clone was digested with *NruI* (1796) and *EcoRI* (0001), and the fragment containing the first five and a half exons of *FA2* was purified by gel extraction. The 5′ and 3′ ends of both the cDNA fragment and genomic clone (lacking the 3′ 1.5 kb) were filled in with T4 DNA polymerase and dNTPs (Invitrogen, Burlington, ON). The ends of the partial genomic clone were dephosphorylated with CIAP (Invitrogen) and then the cDNA fragment was ligated into this genomic clone with T4 DNA ligase (Invitrogen) and transformed into competent DH5α cells. Ampicillin-resistant transformants were assayed for insertion, and clones carrying the correct orientation of the cDNA piece with respect to the genomic piece were identified by restriction digestion. The desired clone would produce a spliced RNA transcript that would be a perfect inverted repeat (Fig. 8A). This primary structure is expected to form a hairpin secondary structure, which is the most efficient trigger for RNAi in plants (Smith et al., 2000) and has been shown to be effective in *Chlamydomonas* (Furhmann et al., 2001).

Molecular characterization of *fa2* mutant alleles

To determine the mutation in each *fa2* allelle, genomic DNA isolated from each mutant strain was amplified by PCR with four sets of primer pairs chosen to span the *FA2* gene in four segments of ~1.2 kb. All products resulting from PCR of *fa2*-2 DNA were of wild-type size and therefore were sequenced in order to identify the mutation. *NIT1* sequence-specific primers were used in combination with *FA2*

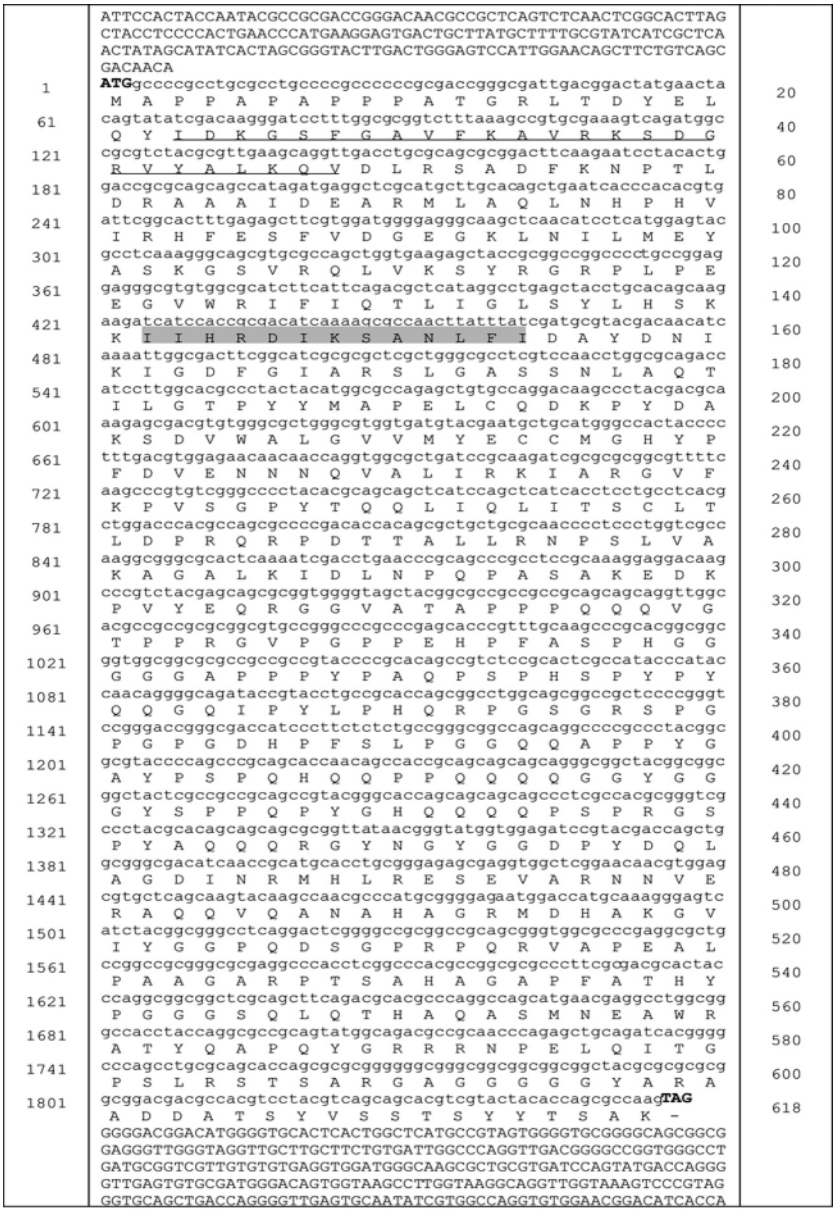

Fig. 1. Nucleotide and deduced amino-acid sequence of *FA2*. Nucleotides are numbered on the left and amino acids on the right. The putative ATP-binding site is underlined and the putative kinase site is shaded. The sequence of *FA2* has been submitted to GenBank under the Accession No. AF479588.

sequence-specific primers to characterize the exogenous DNA insertion in *fa2-1*, *fa2-3* and *fa2-4* because these mutants were generated by insertional mutagenesis. PCR reactions contained 0.5 μM of each primer, 0.5-2.0 μM $MgCl_2$, 0.3 mM dNTP, 1X Taq DNA polymerase buffer, 2.5 U of Taq DNA polymerase (Qiagen, Valencia, CA) and Q solution (for GC rich genomes). PCR mixtures were denatured at 94°C for 2 minutes, followed by 35 cycles of 94°C for 1 minutes, 58-68°C for 1 minute, and 72°C for 1minute followed by a 5 minute extension at 72°C.

Northern analysis

Ten micrograms of polyadenylated RNA was size fractionated on formaldeyhde gels, transferred to Zeta Probe GT membranes (Bio-Rad, Hercules, CA) using 25 mM sodium phosphate (pH 6.4) and fixed using a Stratalinker UV crosslinker (Stratagene). Exon-specific probes, ~0.4 kb to 0.8 kb, were generated with [^{32}P]-dATP or [^{32}P]-dCTP (3000 Ci/mmol) by PCR. Products were purified using the PCR purification kit (Qiagen). Membranes were hybridized with probes at 10^6 cpm/ml at 72°C and washed as described (Virca et al., 1990). Imaging was performed with the Storm system (Molecular Dynamics, Sunnyvale, CA). Before reprobing, blots were stripped using 2×500 mL of 0.5% SDS/0.1× SSC at 94°C for 15 minutes.

Production of *FA1* antibodies and western analysis

The C-terminus of *FA1* (encoding 545 amino acids) was cloned into pGEX-6P-2 (Amersham) and pET28a (Novagen) to produce GST-tagged (GST-Fa1pC) and His-tagged (His-Fa1pC) fusion proteins. Two rabbits were immunized with purified His-Fa1pC protein (Spring Valley Laboratories, Sykesville, MD). Polyclonal anti-sera was affinity purified by standard procedures (Harlow and Lane, 1988), using immobilized GST-Fa1pC (UltraLink Biosupport Medium; Pierce).

For western analysis, flagella-basal body complex protein was isolated as previously described (Lohret et al., 1998). Protein concentration was determined using the Advanced Protein Assay (Cytoskeleton Inc., Denver, CO). Thirty micrograms of protein was separated on a 6% SDS-PAGE gel and electroblotted to supported nitrocellulose (Bio-Rad). To confirm efficient transfer of protein samples, membranes were stained with Ponceau S (Allied Chemicals, Morristown, NJ) and then washed with 0.05% Tween 20 in Tris-buffered saline (TBST). The membrane was blocked in 5% skimmed milk in TBST for 1 hour at room temperature and then incubated overnight at 4°C with anti-Fa1C antibody (at 1:100). The membrane was washed with TBST and incubated with horseradish-peroxidase-linked donkey anti-rabbit Ig (Amersham) at room temperature with rocking for 1 hour. Immunoreactive proteins were visualized using the ECL chemiluminescent detection system (Amersham).

Cell size determination

For cell size measurement, aliquots of cells were centrifuged and resuspended in media containing 2% glutaraldehyde. The sizes of 90-110 cells in randomly selected fields were determined microscopically at 1000× magnification by measuring length (l) and width (w) using software supplied by Motic Images 2000 (Causeway Bay, Hong Kong). Volume was calculated per Umen and Goodenough (Umen and Goodenough, 2001) on the basis of the approximate prolate ellipsoid shape of the cells ($4/3\pi[l/2][w/2]^2$).

Cell division and flow cytometry

Synchronization of cells was carried out as described by Umen and Goodenough (Umen and Goodenough, 2001) with modification. Cultures of wild-type B214 and *fa2* mutant strains were grown in M-media (Harris, 1989) at room temperature with shaking. Flasks were bubbled with 5% CO_2 and grown asynchronously to a density of ~5×10^6 cells/ml in the light, then placed in the dark at 1×10^6 cells/ml for 24 hours. Cultures were then moved back to the light, and aliquots were sampled over the next 24 hours. For each sample, we examined 300 fixed cells microscopically for cleavage furrows

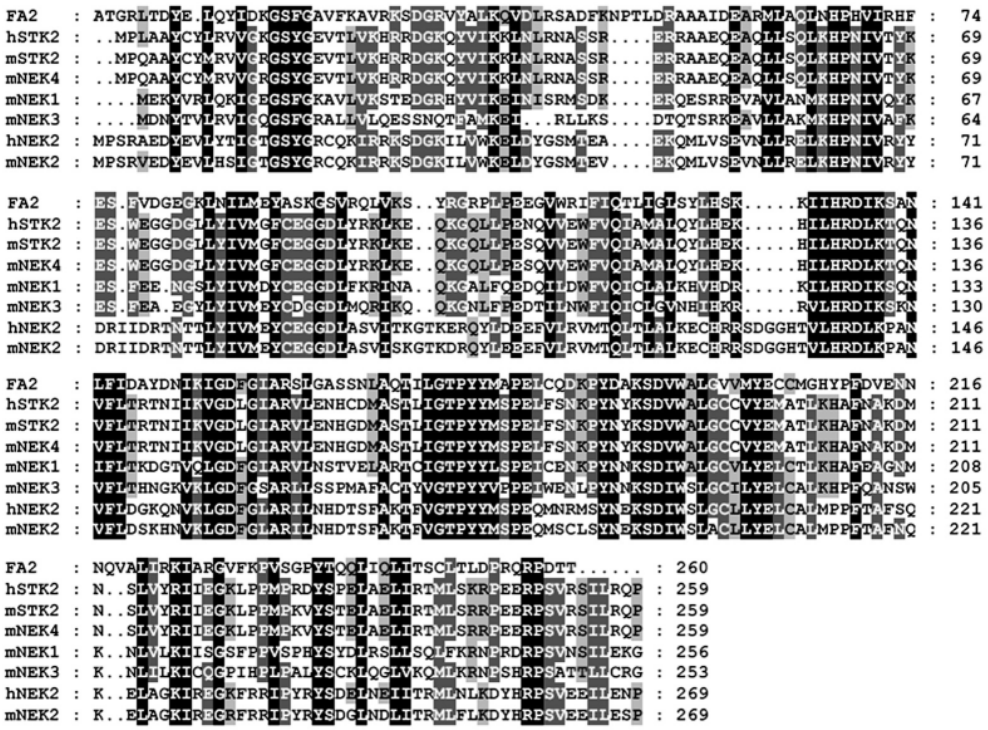

Fig. 2. Amino-acid sequence comparison of Fa2p and other NIMA kinases. The alignment was generated using Clustal W and Genedoc using gaps to maximize homology. Black, dark grey and light grey shading represents 100%, 80% and 60% conservation, respectively. The numbers indicate the relative positions of the amino acids from the N-termini of the various proteins. Sequences used: *Homo sapiens* STK2 (XP_003216.2), *Homo sapiens* Nek2 (NP_002488), *Mus musculus* STK2 (JC7122), *Mus musculus* Nek1 (P51954), *Mus musculus* Nek2 (NP_035022), *Mus musculus* Nek3 (Q9R0A5) and *Mus musculus* Nek4 (NP_035979).

in order to determine the fraction of cells that had entered M phase. In *Chlamydomonas*, incipient cleavage furrows form at pre-prophase and are visible throughout mitosis and cytokinesis (Kirk, 1998). To analyse DNA content, cells were harvested at various times after return to light, collected by centrifugation, resuspended and incubated in 1 volume of 70% ethanol for 1 hour at room temperature. Cells were then prepared for FACS analysis according to a protocol developed by A. Shutz and S. Dutcher (Washington University) as follows. The cells were washed with 1 volume of FACS buffer (0.2M Tris-Cl, pH 7.5, 20 mM EDTA, 5 mM sodium azide) and then resuspended in 0.5 volumes of FACS buffer. 10^6 of these cells were pelleted by centrifugation, resuspended in 100 μL FACS buffer with 1 mg/ml RNase A and incubated for 3 hours at 37°C. Cells were washed with 1mL PBS and then incubated overnight in the dark with 100 μL of PI solution (PBS supplemented with 50 ug/mL propidium iodide; Sigma). To each sample 900 μL of PBS was added. The samples were then analyzed by flow cytometry at the UBC Multiuser FACS Facility (University of British Columbia, Vancouver, Canada).

Results

Cloning the *FA2* gene

The *FA2* allele, *fa2*-3, is a tagged allele that was generated by *NIT1* insertional mutagenesis (Finst et al., 1998). A genomic phage library of *fa2*-3 DNA was screened using probes generated from the transforming DNA. One positive phage clone was identified, and a 1.5 kb *Not*I-*Not*I fragment from this clone, presumed to flank the *FA2* gene, was shown by Southern analysis to hybridize to genomic DNA from wild-type (B214) and all four *fa2* mutant strains (data not shown). We used the 1.5 kb *Not*I fragment to probe a wildtype genomic BAC library of *Chlamydomonas* and identified eight independent positive clones. Only one of these (clone 38g23) was positive by Southern analysis. To determine whether this clone contained the *FA2* gene, the BAC DNA was co-transformed with the selectable marker *NIT1* into *fa2*-2, *nit1*$^-$ mutant cells. We assayed the Nit1$^+$ transformants for deflagellation and identified 17 colonies that rescued the deflagellation defect (~3% of Nit1$^+$ colonies assayed), indicating that the ~70 kb clone, 38g23, did contain the *FA2* gene.

BAC clone 38g23 was digested with various restriction enzymes to identify the smallest fragment of DNA that contained the *FA2* gene. Transformation of *fa2* mutants with these fragments lead to the identification of a 4.6 kb *Sac*I-*Sal*I fragment that rescued the deflagellation defect in *fa2-1* and *fa2-2* (21 rescues out of 1108 transformants assayed; ~2%). Southern analysis showed that the 4.6 kb insert was present in wild-type cells and transformation-rescued *fa2-1* cells but not in *fa2-1* mutant cells (data not shown). Because the 4.6 kb fragment rescues the deflagellation defect, and because it physically maps to the *FA2* locus, we concluded that it contains the *FA2* gene. The rescuing clone was sequenced, and seven putative exons were identified by the Genemark gene prediction algorithm. This prediction was used to design primers for RT-PCR and 3′ RACE of polyadenylated RNA isolated from wild-type cells. DNA sequencing and subsequent alignment of the cDNA clone with the genomic sequence confirmed the seven exons and defined the 5′ and 3′ untranslated regions. The cDNA sequence was used by C. Silflow and M. LaVoie (University of Minnesota) to map the *FA2* gene to linkage group VII (Vysotskaia et al., 2001).

FA2 encodes a Nek kinase

The *FA2* cDNA encodes 618 amino acids with a predicted molecular mass of 68 kDa (Fig. 1). Searches of public databases identified many proteins in the NIMA family of expressed kinases (Neks), with high amino acid identity (35-

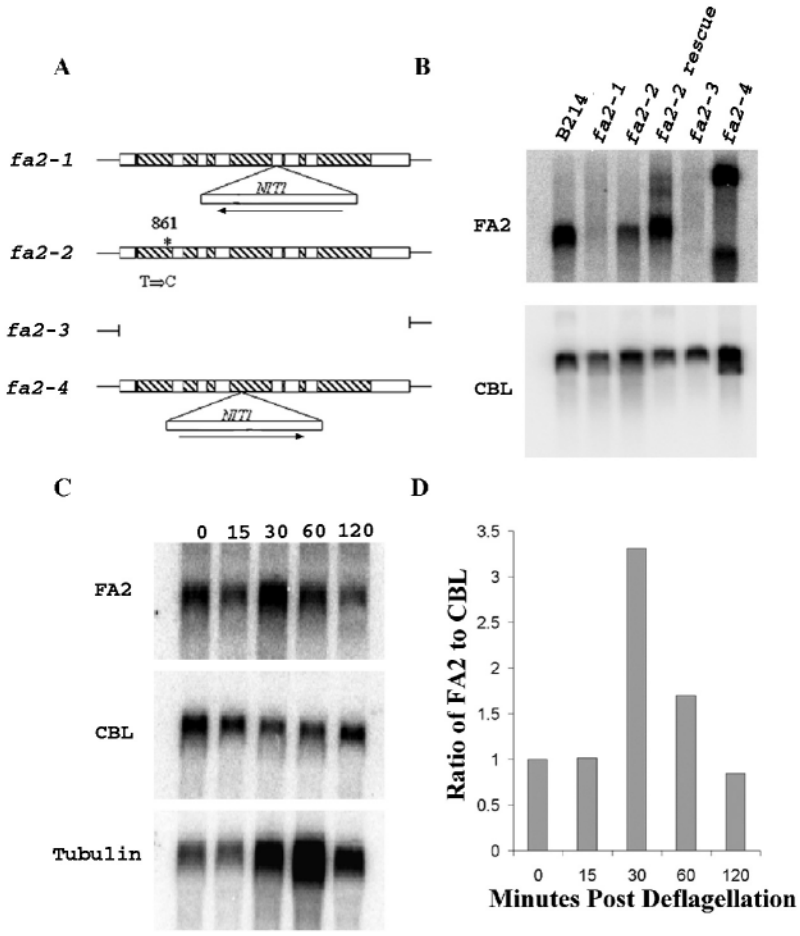

Fig. 3. Northern analysis of *FA2* gene and the *fa2* mutant alleles. (A) Schematic representation of the mutant alleles. *fa2*-1, *fa2*-3 and *fa2*-4 were generated by NIT1 insertion and *fa2*-2 was generated by UV mutagenesis (see Finst et al., 1998). (B) Ten micrograms of polyadenylated RNA from log phase cells was loaded per lane. The blot was probed with 0.7 kb of *FA2* cDNA, and re-probed with 0.5 kb of the *CBL* gene as a loading control. (C) Northern analysis of RNA from wild-type cells following deflagellation by pH shock (Witman et al., 1972). Each lane contains 10 μg of polyadenylated RNA taken at the indicated time post deflagellation. The blot was probed with 0.7 kb of *FA2* cDNA and re-probed with 0.5 kb of *CBL* cDNA and 0.5 kb of β-tubulin cDNA as controls. (D) Ratio of *FA2* message compared with that of CBL.

40%) to *FA2* in the N-terminal kinase domain (Fig. 2). The motif (IKSAN) in the catalytic domain suggests that Fa2p is a serine/threonine kinase (Fig. 2) (Hanks et al., 1991). Little or no sequence similarity exists in the C-terminal regions of these proteins, but, like several other Neks, the C-terminal region of Fa2p is basic (pI 9.6) (Wang et al., 1998). Phylogenetic analysis using the complete Fa2p amino-acid sequence or N-terminal domain showed that Fa2p is a NIMA kinase member but failed to tightly associate Fa2p with a specific subfamily of NIMA kinases (data not shown).

Characterizing the *fa2* mutant alleles

PCR analysis and sequencing of the three mutant alleles generated by *NIT1* insertion revealed an insertion in the fourth intron of *fa2*-1 and an insertion in the fourth exon of *fa2*-4 (Fig. 3A.). By Southern analysis, *FA2* is completely deleted in *fa2*-3 (data not shown). The UV-generated allele, *fa2*-2, has a C to T transition at position 861bp, causing a codon change from glutamine to a stop codon (Fig. 3A).

Northern analysis showed a wild-type transcript of ~3.0 kb, which was not detected in *fa2*-1 or *fa2*-3 cells, demonstrating that FA2 is not an essential gene (Fig. 3B). The *fa2*-4 strain produces a message of ~8.7 kb, consistent with the insertion of *NIT1* (Fig. 3B). The UV-generated mutant, *fa2*-2, expressed a transcript of the correct size, but at a lower level than that of wild-type cells. *fa2-2* cells rescued for deflagellation by transformation with the 4.6 kb subclone express wild-type levels of *FA2* message (Fig. 3B).

Patterns of FA2 expression

By northern analysis, we discovered that *FA2* mRNA levels increase approximately 3.5-fold 30 minutes post deflagellation compared with CBL, a constitutively expressed message (Schloss, 1990), and return to normal expression levels by 60 minutes (Fig. 3C,D). The peak of *FA2* expression occurs more rapidly than peak expression of the highly up-regulated tubulin (Fig. 3C) (Schloss et al., 1984).

Fa1p is localized to the flagellar transition zone in *fa2* mutants

We have previously used isolated, de-membranated, flagellar-basal body complexes (FBBCs) for the in vitro assay of axonemal microtubule severing (Lohret et al., 1999). Therefore, to test whether Fa2p might affect the targeting of proteins to the axonemal severing complex, the localization of Fa1p to FBBCs was examined in *fa2* cells. Fa1p is essential for axonemal microtubule severing and localizes to the basal body/flagellar transition region (Finst et al., 2000). This localization appears to be unaltered in the *fa2* mutants (Fig. 4). Therefore, it is likely that Fa2p is doing something other than facilitate localization of the axonemal

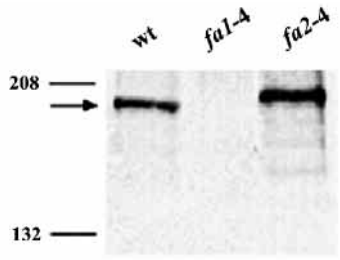

Fig. 4. Localization of Fa1p in *fa2* mutant cells. Western blot of flagellar-basal body complexes (FBBCs) isolated from wild-type, *fa1*-4 and *fa2*-4 strains. Thirty micrograms of protein were loaded into each lane and the blot was probed with a polyclonal antibody recognizing the C-terminus of *FA1*.

microtubule severing complex to the flagellar transition zone.

Some *fa2* mutant cells are larger than wild-type cells

We noticed that *fa2* cells were larger than wild type (Fig. 5A). This was quantified by measuring volumes of wild-type, *fa2* mutant and *fa2*-2-rescue strains. Two independent examinations of asynchronous populations of cells confirmed that there is a difference in mean volume of wild-type (151 μm^3) and *fa2* mutant cells (*fa2*-2, 287 μm^3; *fa2*-3, 257μm^3; *fa2*-4, 214 μm^3). The *fa2*-2-rescue strain regained a wild-type cell volume (152 μm^3). The size distribution of mutants and wild-type cells was also strikingly different (Fig. 5B). This difference in cell size distribution could reflect faster rates of *fa2* cell growth relative to wild type or a delay in cell cycle progression, providing *fa2* cells more time to grow before cell division. To distinguish these possibilities, we examined cell growth in synchronized populations.

Chlamydomonas uses a multiple fission mechanism of cell division (Pickett-Heaps, 1975). Vegetative cells can grow to many times their original size during a prolonged G1 phase. There is a point during G1, called 'commitment', when cells that have achieved a minimal cell volume will commit to at least one round of cell division even in the absence of further growth (larger cells will undertake multiple rounds of division) (Pickett-Heaps, 1975; Spudich and Sager, 1980). Subsequently, the cells undergo multiple rounds of rapidly alternating S and M phases, producing 2, 4, 8 or 16 daughter cells of equal size (Coleman, 1982; Craigie and Cavalier-Smith, 1982; Donnan and John, 1983).

In asynchronous populations grown in continuous light, *fa2* cells are larger than wild-type cells (Fig. 5). When these same cultures are placed in the dark for 24 hours there is no further cell growth, and cells that were larger than commitment minimum when placed in the dark will divide to produce daughter cells (which then join the population of cells below the threshold size for division). After 24 hours in the dark, all cells larger than the commitment threshold are expected to have divided. Thus the maximum cell size after 24 hours in the dark should correspond approximately to the commitment threshold. Wild-type and *fa2* mutant cells showed no difference in the maximum cell size after 24 hours in the dark (Fig. 6A). Furthermore, the size threshold was comparable to that previously reported for wild-type cells (178 μm^3) (Umen and Goodenough, 2001). This indicates that *fa2* cells are not defective in the coupling of cell size to commitment and provides an opportunity to assess rates of cell growth after return to the light. Fig. 6A shows that 10 hours after a shift into the light, both populations of cells increased in mean volume; *fa2* cells did not grow faster than wild-type cells. In contrast to the disparate size distributions observed for asynchronous cultures of *fa2* and wild-type cells, populations within the first 10 hours of return to growth conditions show similar distributions (compare Fig. 5 with Fig. 6A). In asynchronous populations *fa2* cells are on average larger than wild-type cells, but the cells seem to grow at the same rate and have a similar size threshold for commitment to divide. These data lead us to predict that the larger *fa2* cells would, on average, undergo more rounds of fission per division cycle than wild-type cells. As shown in Fig. 6B, this is what we observed. In other words, the larger *fa2* cells are dividing into more daughter cells, thus producing a spectrum of cell size comparable to wild type after 24 hours in the dark, when all cells above the threshold will have divided. On the basis of these data, we hypothesized that *fa2* cells are slow to transit through the cell cycle. This would provide more time for growth, allowing the cells to grow larger, followed by an increased number of fission events, producing daughter cells of wild-type size.

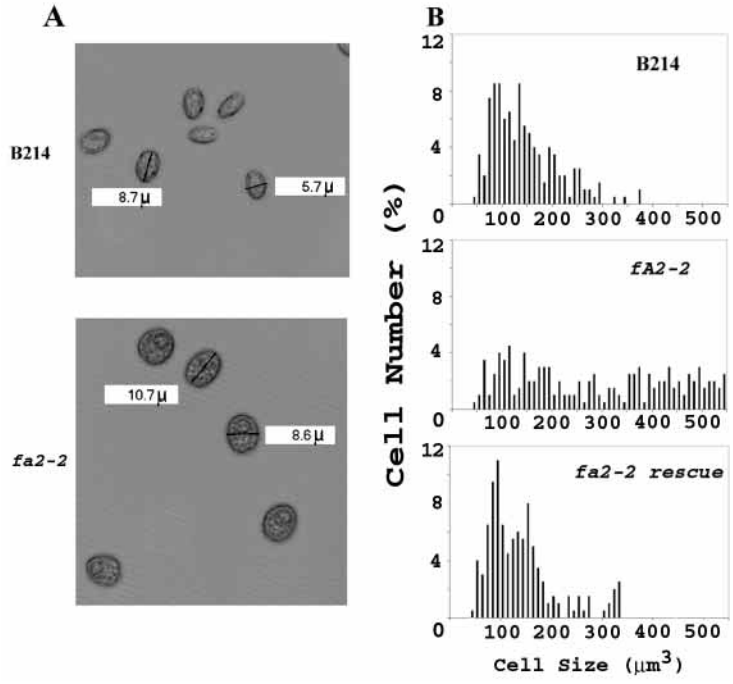

Fig. 5. Cell size distribution of log phase cells. (A) Photomicrographs of wild-type (B214) and *fa2*-2 cells. The *fa2*-2 cells are larger (on average) with respect to length, width and volume. (B) Size distribution of wild-type, *fa2*-2 and *fa2*-2 rescued cells. Cell volumes were calculated from length and width measurements as described in Materials and Methods. The mean volumes were: wild type (151 μm^3), *fa2*-2 (287 μm^3) and *fa2*-2 rescued (152 μm^3). One hundred cells from each culture were measured.

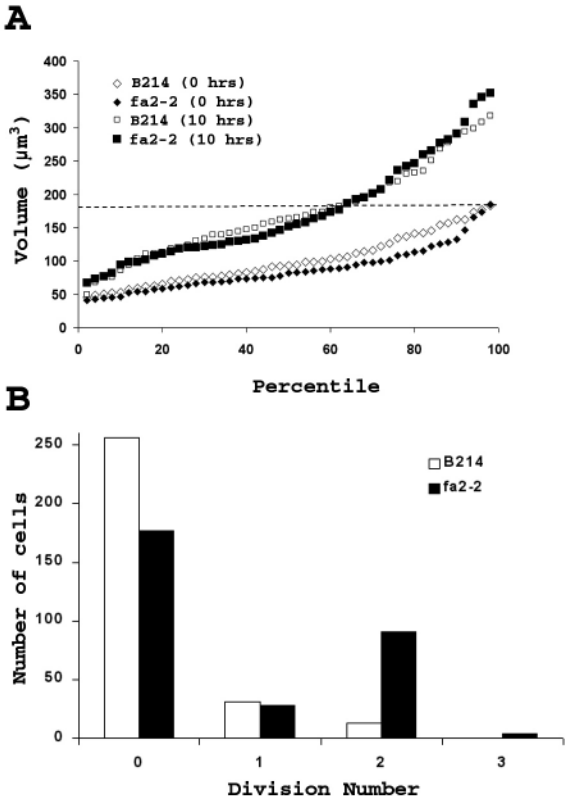

Fig. 6. Cell size distribution of synchronized cells and multiple fission of asynchronous cells. (A) Wild type and *fa2*-2 mutant cells were grown in minimal media for several days in constant light, then placed in the dark for 24 hours. Cell sizes were measured immediately following exposure to light and again after 10 hours of continuous light. One hundred cells from each culture were measured. (B) Wild-type and *fa2*-2 mutant cells were grown in rich (TAP) media in constant light for several days. Aliquots of the culture were plated on minimal media and placed in the dark for 24 hours. Individual cells/colonies were scored for having undergone 0, 1, 2, 3 or 4 divisions during the 24 hour incubation in the dark by counting cells in micro-colonies. 300 cells were scored for each culture from each of two independent experiments.

fa2 mutant cells are slow to progress through the cell cycle

In order to compare the rate of progression of *fa2* and wild-type cells through the cell cycle, we measured DNA content and assessed the division status of cells returned to the light after 24 hours in the dark. Mitotic figures and the mitotic spindle are difficult to visualize in *Chlamydomonas*, thus we choose to use the readily visible cleavage furrows to identify cells in M phase. Cleavage furrows are first visible in pre-prophase and persist through cytokinesis, they therefore provide a good indication of cells in mitosis (Kirk, 1998).

We sampled cells immediately after return to light (0 hours of continuous light) and then again after 10 hours and 21 hours in continuous light. After 24 hours in the dark, wild-type and *fa2* cells have similar distributions of DNA per cell. Ten hours after return to the light, both populations increased their DNA content to the same extent, indicating that S phase is not delayed in the *fa2* mutant. By 21 hours in the light, a significant fraction of the wild-type population has undergone cytokinesis and hatched from the mother cell wall, yielding cells of 1N. In contrast, the *fa2* cells had not hatched at the 21 hour time point (Fig. 7). Apparently, the *fa2* cells take longer to transit from G2 through mitosis and cytokinesis to hatch as individual cells of 1N.

A count of cells with cleavage furrows indicates that *fa2* cells are slower to enter M phase (Fig. 7E). Fig. 7A and 7C shows that *fa2* cells complete S phase in synchrony with wild-type cells, yet Fig. 7E shows that they are slower to enter mitosis. We conclude from this that *fa2* mutant cells are delayed at the G2/M transition. But this is clearly not the only point in the cell cycle where *fa2* cells are slower than wild-type cells. A comparison of Fig. 7B and 7D illustrates that *fa2* cells are also slow to return to 1N. Microscopic examination of these samples revealed that the delay in return to 1N was in large part caused by failure of the daughter cells to hatch from the mother cell wall (daughter cells, held together by the mother cell wall, were counted as single particles by the FACS machine). Flagella-less cells often have difficulty hatching from the mother cell wall; therefore, we digested the mother walls from these cells. We discovered that the daughter cells had not yet assembled flagella (data not shown). We have also

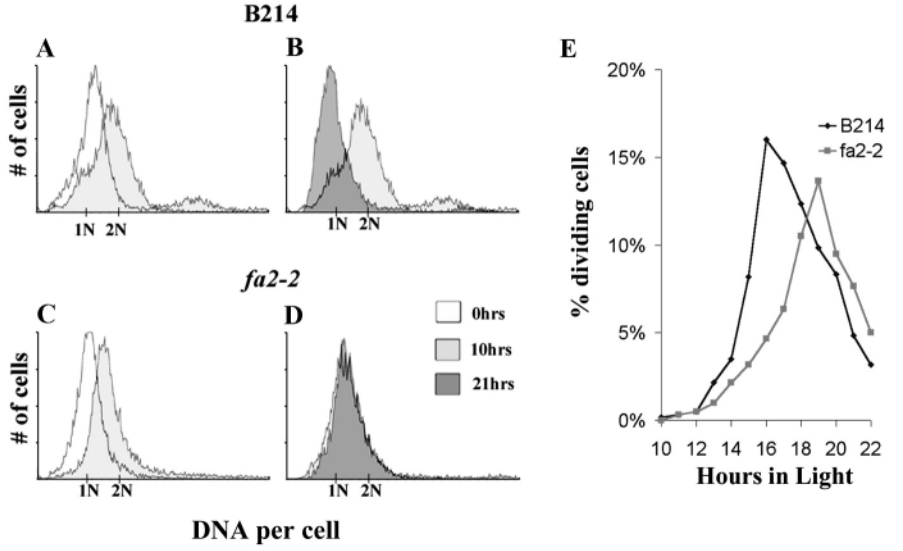

Fig. 7. Cell cycle analyses. (A-D) FACS analysis of synchronized wild-type and *fa2*-2 cultures. Cells were synchronized by incubation in the dark for 24 hours. Samples were taken at 0, 10 and 21 hours after return to the light and prepared for flow cytometric analysis. DNA content per cell, measured by fluorescence intensity of incorporated propidium iodide, is plotted in a histogram depicting relative cell numbers at each intensity. (E) Cultures were incubated in the dark for 24 hours and then returned to the light. Aliquots were then analyzed microscopically at the indicated time points for evidence of mitotic cleavage furrows. The percentage of cells with cleavage furrows was scored as the % of cells in M phase. Three hundred cells were scored for each culture.

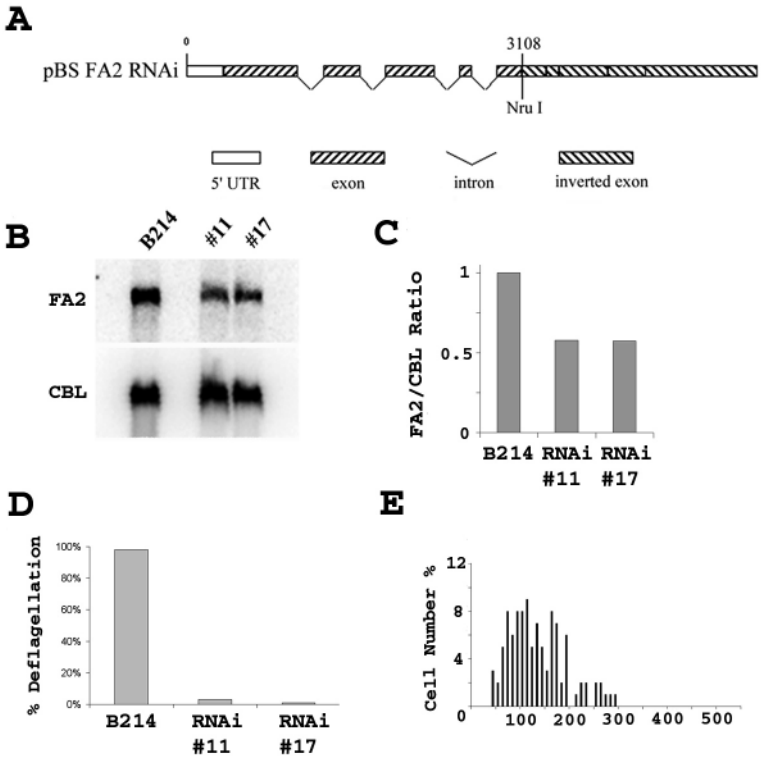

Fig. 8. RNAi of *FA2* in wild-type *Chlamydomonas* cells. (A) Construct for triggering RNAi. The construct pBSFA2-RNAi was created by cloning a cDNA cassette containing exons 1 to 5 in inverse orientation at the 3′ end of the corresponding genomic DNA. (B) Northern analysis of *FA2* in cells transformed with the pBSFA2-RNAi construct. Each lane contains 10 μg of polyadenylated RNA obtained from a population of asynchronous cells from the strain indicated. The blot was probed with 0.7 kb of *FA2* cDNA and re-probed with 0.5kb of *CBL* as a loading control. (C) Ratio of FA2 mRNA signal compared with that of CBL. (D) Deflagellation response of each cell type to acid. (E) Cell size distribution of RNAi colony number 17. One hundred cells were measured.

observed that in rich (TAP) media, rapidly growing asynchronous populations of *fa2* cells accumulate clusters of flagella-less daughter cells. We conclude that *fa2* mutant cells are delayed at the G2/M transition and in the assembly of flagella after exit from mitosis.

RNAi of *FA2* mimics deflagellation but not cell size profile of *fa2* mutants

RNA interference (RNAi) is a mechanism of gene silencing that has been shown to be effective in a wide range of organisms (Smith et al., 2000). One approach to RNAi involves introduction of a gene construct which, following transcription in vivo, produces a hairpin dsRNA. Recently, this method has been shown to be an effective way of reducing the function of a target gene in *Chlamydomonas* (Furhmann et al., 2001). Because all of our *fa2* alleles are probably null (Fig. 3A,B), RNAi was used to generate strains of *Chlamydomonas* with reduced expression of *FA2*. To generate a DNA construct that would produce a hairpin dsRNA, exons 1 to 5 of the cDNA were inverted and ligated to ~3 kb of the *FA2* genomic fragment representing the same exons (Fig. 8A). This construct was co-transformed with the selectable marker *Ble* into wildtype cells. Cells that acquired resistance to Zeocin were assayed for a deflagellation phenotype. We found that 18/121 Zeocin-resistant strains were defective for deflagellation. Specifically, they were defective in calcium-induced axonemal severing assayed as previously described (Fig. 8D) (Finst et al., 2000). Two of these strains were examined by northern analysis and both showed two-fold reductions in levels of *FA2* mRNA (Fig. 8B,C). Surprisingly, the cell size distribution of the RNAi strains was the same as wild type (Fig. 8E). From these data we infer that the deflagellation phenotype is sensitive to *FA2* expression levels, whereas the cell size phenotype is less sensitive. However, when grown asynchronously in rich media, the RNAi cells, like the *fa2* mutants, are slow to form flagella and hatch from the mother cell wall. The high sensitivity of deflagellation to *FA2* expression levels is consistent with the low rates of co-transformation that we achieve in deflagellation transformation rescue experiments with *FA2* (1-3% compared to 10-15% for *FA1*) (Finst et al., 2000).

Discussion

Mutations in the *FA2* gene of *Chlamydomonas* cause defects in calcium-induced axonemal microtubule severing (Finst et al., 1998). We have determined that *FA2* encodes a NIMA family kinase that is not essential for viability. We have shown that all four *fa2* alleles contain mutations in the *FA2* gene (Fig. 3A,B): *fa2*-2 has a nonsense mutation in the first exon; the *FA2* gene is disrupted by a *NIT1* insertion in two alleles, *fa2*-1 and *fa2*-4; and the *FA2* gene is completely deleted in *fa2*-3. We have rescued three of these strains by transformation with the genomic clone. In addition, we have shown that a 50% reduction in *FA2* mRNA, induced by RNAi, results in an axonemal severing defect (Fig. 8). We conclude that the gene we have cloned is *FA2*. Therefore, a member of the Nek kinase protein family plays an essential role in signal-induced severing of axonemal microtubules during the deflagellation behaviour of *Chlamydomonas*.

As we observed previously for the *FA1* gene (Finst et al., 2000) and for katanin p60 (T. A. Lohret and L.M.Q., unpublished), *FA2* mRNA levels are modestly increased during flagellar regeneration (Fig. 3C,D). These data suggest that katanin, Fa1p and Fa2p are components of the flagella or play a role in the assembly of new flagella. We previously showed that Fa1p is localized to the basal body/flagellar transition zone (Finst et al., 2000), and we show here that this localization is

not disrupted in *fa2* mutants (Fig. 4). This would indicate that Fa2p is not essential for the localization of Fa1p.

In addition to the axonemal-severing defect, we have discovered that *fa2* mutants have subtle cell cycle progression defects. Populations of asynchronously growing *fa2* cells have a cell volume distribution that encompasses the wild-type spectrum but also extends to include cells that are almost twice as large as any seen in the wild-type populations (Fig. 5). When the populations are partially synchronized, *fa2* cells grow at approximately the same rate as wild-type cells (Fig. 6A), suggesting that *fa2* cells are probably larger because they grow for a longer time before completing cell division. We suggest that this may be because of a delay in transit through the cell cycle.

Analyses of DNA content and cell division support the idea that *fa2* cells are delayed in transit through at least two points in the cell cycle: (1) the G2/M transition and (2) in the assembly of flagella after exit from mitosis. However, the role of Fa2p at each of these points must be non-essential because *fa2* mutant cells do transit the cell cycle, albeit more slowly than wild-type cells. It is possible that other Nek family members in *Chlamydomonas* compensate for the cell cycle functions of Fa2p in the *fa2* mutants. We have identified two related proteins in the *Chlamydomonas* EST database.

Our discovery that *FA2* encodes a Nek kinase is the first indication that this family might play a role in the regulation of microtubule severing. It is also possible that the axonemal severing defect of *fa2* mutants is a secondary consequence of defective centrosome/basal body assembly. During cell division in *Chlamydomonas*, the flagella are resorbed and the basal bodies function as centrioles, providing foci for the spindle poles (for a review, see Kirk, 1998). When division is complete the centrioles reposition as basal bodies and new flagella are assembled. On the basis of our observation that flagellar assembly is delayed in *fa2* mutants, and the report that Nek2 facilitates centrosome assembly (Fry et al., 2000), we speculate that Fa2p might play a role in the centriole cycle in *Chlamydomonas*. For example, a delay in the differentiation of centrioles into basal bodies would translate as a delay in flagellar assembly, which in turn would cause a delay in hatching from the mother cell wall. Furthermore, the calcium-induced axonemal microtubule-severing defect of *fa2* mutants is associated with mature basal bodies and therefore this too may be a consequence of defective centriole differentiation. One piece of evidence that argues against a role for Fa2p in assembly of specific centrosome/basal-body-associated complexes is the observation that Fa1p, whose only known function is its essential role in calcium-induced axonemal microtubule severing, retains its localization to the basal body/transition zone in *fa2* mutant.

Fa2p function, as it relates to both deflagellation and cell cycle progression, might be directly related to microtubule severing associated with the basal body/centriole. Microtubule severing has been implicated in cell cycle progression (for a review, see Quarmby, 2000), and it is possible that both the deflagellation and cell cycle phenotypes of *fa2* mutants are related to defects in microtubule severing, directly or indirectly. Future experiments will discriminate whether the cell cycle progression defect of *fa2* cells is a consequence of a microtubule severing defect or a hampered centrosomal cycle. Most intriguing is the possibility that microtubule severing plays a role in the centrosomal cycle.

We thank Peter J. Kim and Christina Ames for assistance with some of the experiments. We are grateful to Susan Dutcher (Washington University, USA) and Fiona Brinkman (Simon Fraser University, Canada) for productive discussions, Peter Hegemann (University of Regensburg, Germany) for sharing data prior to publication, Carolyn Silflow and Matthew LaVoie (University of Minnesota, USA) for physical mapping of the *FA2* gene, and Peter Unrau (Simon Fraser University, Canada) for the use of his phosphoimager. Financial support for this work was provided by operating grants to LMQ from the Natural Sciences and Engineering Research Council of Canada (RGPIN 227132) and the Canadian Institutes of Health Research (MOP 37861).

References

Ahmad, F. J., Yu, W., McNally, F. J. and Baas, P. W. (1999). An essential role for katanin in severing microtubules in the neuron. *J. Cell Biol*. **145**, 301-315.

Altschul, S. F., Madden, T. L., Schäffer, A. A., Zhang, J., Zhang, Z., Miller, W. and Lipman, D. J. (1997). Gapped BLAST and PSI- BLAST: a new generation of protein database search programs. *Nucleic Acids Res*. **25**, 3389-3402.

Belham, C., Comb, M. J. and Avruch, J. (2001). Identification of the NIMA family of kinases NEK6/7 as regulators of the p70 ribosomal S6 kinase. *Curr. Biol.* **11**, 1155-1167.

Benian, G., Tinley, T. L., Tang, X. and Borodovsky, M. (1996). The *C. elegans* gene unc-89, required for muscle M-line assembly, encodes a giant modular protein composed of Ig and signal transduction domains. *J. Cell Biol.* **6**, 835-848.

Brinkman, F. S. L., Wan, I., Hancock, R. E. W., Rose, A. M. and Jones, S. J. (2001). PhyloBLAST: facilitating phylogenetic analysis of BLAST results. *Bioinformatics* **17**, 385-387.

Coleman, A. W. (1982). The nuclear cell cycle in *Chlamydomonas* (Chlorophyceae). *J. Phycol*. **18**, 192-195.

Craigie, R. A. and Cavalier-Smith, T. (1982). Cell volume and the control of the *Chlamydomonas* cell cycle. *J. Cell Sci*. **54**, 173-191.

Debuchy, R., Purton, S. and Rochaix, J. D. (1989). The argininosuccinate lyase gene of *Chlamydomonas reinhardtii*: an important tool for nuclear transformation and for correlating the genetic and molecular maps of the ARG7 locus. *EMBO J.* **8**, 2803-2809.

Donnan, L. and John, P. C. (1983). Cell cycle control by timer and sizer in *Chlamydomonas*. *Nature* **304**, 630-633.

Felsenstein, J. (1989). PHYLIP – Phylogeny Inference Package (Version 3.2). *Cladistics* **5**, 164-166.

Fernandez, E., Schnell, R., Ranum, L. P. W., Hussey, S. C., Silflow, C. D. and Lefebvre, P. A. (1989). Isolation and characterization of the nitrate reductase structural gene of *Chlamydomonas reinhardtii*. *Proc. Natl. Acad. Sci. USA* **86**, 6449-6453.

Finst, R. J., Kim, P. J. and Quarmby, L. M. (1998). Genetics of the deflagellation pathway in *Chlamydomonas reinhardtii*. *Genetics* **149**, 927-936.

Finst, R. J., Kim, P. J., Griffiths, P. R. and Quarmby, L. M. (2000). Fa1p is a 171 kDa protein essential for axonemal microtubule severing in *Chlamydomonas*. *J. Cell Sci*. **113**, 1963-1971.

Fry, A. M. and Nigg, E. A. (1995). The NIMA kinase joins forces with Cdc2. *Curr. Biol.* **5**, 1122-1125.

Fry, A. M., Mayor, T., Meraldi, P., Stierhof, Y. D., Tanaka, K. and Nigg, E. A. (1998). C-Nap, a novel centrosomal coiled-coil protein and candidate substrate of the cell cycle-regulated protein kinase Nek2. *J. Cell Biol*. **141**, 1563-1574.

Fry, A. M., Descombes, P., Twomey, C., Bacchieri, R. and Nigg, E. A. (2000). The NIMA-related kinases X-Nek2B is required for efficient assembly of the zygotic centrosome in *Xenopus laevis*. *J. Cell Sci.* **113**, 1973-1984.

Fuhrmann, M., Stahlberg, A., Govorunova, E., Rank, S. and Hegemann, P. (2001). The abundant retinal protein of the *Chlamydomonas* eye is not the photoreceptor for phototaxis and photophobic responses. *J. Cell Sci.* **114**, 3857-3863.

Hanks, S. K. and Quinn, A. M. (1991). Protein kinase catalytic domain

sequence database: identification of conserved features of primary structure and classification of family members. *Methods Enzymology* **200**, 38-62.

Harlow, E. and Lane, D. (1998). Antibodies: A Laboratory Manual. Cold Spring Harbor Laboratory Publications: New York.

Harris, E. H. (1989). The *Chlamydomonas* Sourcebook. Berkeley, CA: Academic Press.

Hayashi, K., Igarashi, H., Ogawa, M. and Sakaguchi, N. (1999). Activity and substrate specificity of the murine STK2 serine/threonine kinase that is structurally related to the mitotic regulator protein NIMA of *Aspergillus nidulans*. *Biochem. Biophys. Res. Commun.* **264**, 449-456.

Kirk, D. L. (1998). Volvox. Molecular-genetic origins of multicellularity and cellular differentiation. New York, NY: Cambridge University Press.

Lohret, T. A., McNally, F. J. and Quarmby, L. M. (1998). A role for katanin-mediated axonemal severing during *Chlamydomonas* deflagellation. *Mol. Biol. Cell* **9**, 421-437.

Lohret, T. A., Zhao, L. and Quarmby, L. M. (1999). Cloning of *Chlamydomonas* p60 katanin and localization to the site of outer doublet severing during deflagellation. *Cell Motil. Cytoskeleton* **43**, 221-231.

Lu, K. P. and Means, A. R. (1994). Expression of the non-cataytic domain of the NIMA kinase causes a G2 arrist in *Aspergillus nidulans*. *EMBO J.* **13**, 2103-2113.

Mayor, T., Stierhof, Y. D., Tanaka, K., Fry, A. M. and Nigg, E. A. (2000). The centrosomal protein C-Nap1 is required for cell cycle-regulated centrosome cohesion. *J. Cell Biol.* **151**, 837-846.

McNally, F. J. and Thomas, S. (1998). Katanin is responsible for the M-phase microtubule-severing activity in *Xenopus* eggs. *Mol. Biol. Cell* **9**, 1847-1861.

McNally, F. J., Okawa, K., Iwamatsu, A. and Vale, R. D. (1996). Katanin, the microtubule-severing ATPase, is concentrated at centrosomes. *J. Cell Sci*. **109**, 561-567.

McNally, K. P., Bazirgan, O. A. and McNally, F. J. (2000). Two domains of p80 katanin regulate microtubule severing and spindle pole targeting by p60 katanin. *J. Cell Sci*. **113**, 1623-1633.

Morris, N. R. (1976). Mitotic mutants of *Aspergillus nidulans*. *Genet. Res.* **26**, 237-254.

Nicholas, K. B., Nicholas H. B., Jr. and Deerfield, D. W., II (1997). GeneDoc: Analysis and visualization of genetic variation. *EMBNEW NEWS* **4**, 14.

O'Connell, M. J., Norbury, C. and Nurse, P. (1994). Premature chromatin condensation upon accumulation of NIMA. *EMBO J*. **13**, 4926-4937.

Odde, D. J., Ma, L., Briggs, A. H., DeMarco, A. and Kirschner, M. W. (1999). Microtubule bending and breaking in living fibroblast cells. *J. Cell Sci.* **112**, 3283-3288.

Osmani, S. A., Pu, R. T. and Morris, N. R. (1988). Mitotic induction and maintenance by overexpression of a G_2-specific gene that encodes a potential protein kinase. *Cell* **53**, 237-244.

Osmani, A. H., McGuire, S. L. and Osmani, S. A. (1991). Parallel activation of the NIMA and p34cdc2 cell cycle-regulated protein kinases is required to initiate mitosis in *A. nigulans*. *Cell* **67**, 283-291.

Pickett-Heaps, J. D. (1975). Green Algae. Sinauer Associates, Sunderland, MA.

Quarmby, L. M. (1996). Calcium influx activated by low pH in *Chlamydomonas*. *J. Gen. Physiol.* **108**, 351-361.

Quarmby, L. M. (2000). Cellular samurai: katanin and the severing of microtubules. *J. Cell Sci*. **113**, 2821-2827.

Rhee, K. and Wolgemuth, D. J. (1997). The NIMA-related kinase 2, Nek2, is expressed in specific stages of the meiotic cell cycle and associates with meiotic chromosomes. *Development* **124**, 2167-2177.

Rodionov, V., Nadezhdina, E. and Borisy, G. (1999). Centrosomal control of microtubule dynamics. *Proc. Natl. Acad. Sci. USA* **96**, 115-120.

Sager, R. and Granick, S. (1953). Nutritional studies with *Chlamydomonas reinhardtii*. *Ann. NY Acad. Sci.* **56**, 831-838.

Schloss, J. A., Silflow, C. D. and Rosenbaum, J. L. (1984). mRNA abundance changes during flagellar regeneration in *Chlamydomonas reinhardtii*. *Mol. Cell. Biol.* **4**, 424-434.

Schloss, J. A. (1990). A *Chlamydomonas* gene encodes a G protein beta subunit-like polypeptide. *Mol. Gen. Genet.* **221**, 443-452.

Smith, N. A., Singh, S. P., Wang, M.-B., Stoutjesdijk, P. A., Green, A. G. and Waterhouse, P. M. (2000). Gene expression: Total silencing by intron-spliced hairpin RNAs. *Nature* **407**, 319-320.

Spudich, J. L. and Sager, R. (1980). Regulation of *Chlamydomonas* cell cycle by light and dark. *J. Cell Biol*. **85**, 136-145.

Srayko, M., Buster, D. W., Bazirgan, O. A., McNally, F. J. and Mains, P. E. (2000). MEI-1/MEI-2 katanin-like microtubule severing activity is required for *C. elegans* meiosis. *Genes Dev.* **14**, 1072-1084.

Tanaka, K., Parvinen, M. and Nigg, E. A. (1997). The in vivo expression pattern of mouse Nek2, a NIMA-related kinase, indicates a role in both mitosis and meiosis. *Exp. Cell Res.* **237**, 264-274.

Thompson, J. D., Higgins, D. G. and Gibson, T. J. (1994). CLUSTAL W: improving the sensitivity of progressive multiple sequence alignment through sequence weighting, position-specific gap penalties and weight matrix choice. *Nucleic Acids Res*. **22**, 4673-4680.

Umen, J. G. and Goodenough, U. W. (2001). Control of cell division by a retinoblastoma protein homolog in *Chlamydomonas*. *Genes Dev.* **15**, 1652-1661.

Upadhya, P., Birkenmeier, E. H., Birkenmeier, C. S. and Barker, J. E. (2000). Mutations in a NIMA-related kinase gene, *Nek1*, cause pleiotropic effects including a progressive polycystic kidney disease in mice. *Proc. Natl. Acad. Sci. USA* **97**, 217-221.

Virca, G. D., Northemann, W., Sheils, B. R., Widera, G. and Broome, S. (1990). Simplified northern blot hybridization using 5% sodium dodecyl sulfate. *Biotechniques* **8**, 370-371.

Vysotskaia, V. S., Curtis, D. E., Voinov, A. V., Kathir, P., Silflow, C. D. and Lefebvre, P. A. (2001). Development and characterization of genome-wide single nucleotide polymorphism markers in the green alga *Chlamydomonas reinhardtii. Plant Physiol*. **127**, 386-389.

Wang, S., Nakashima, S., Sakai, H., Numata, O., Fujiu, K. and Nozawa, Y. (1998). Molecular cloning and cell-cycle-dependant expression of a novel NIMA (never-in-mitosis) related protein kinase (*Tp*NRK) in *Tetrahymena* cells. *Biochem. J*. **334**, 197-203.

Waterman-Storer, C. M. and Salmon, E. D. (1997). Actomyosin-based retrograde flow of microtubules in the lamella of migrating epithelial cells influences microtubule dynamic instability and turnover and is associated with microtubule breakage and treadmilling. *J. Cell Biol*. **139**, 417-434.

Witman, G. B., Carlson, K., Berliner, J. and Rosenbaum, J. L. (1972). Isolation and electrophoretic analysis of microtubules, membranes and mastigonemes. *J. Cell Biol*. **54**, 507-539.

Wu, L., Osmani, S. A. and Mirabito, P. M. (1998) A role for NIMA in the nuclear localization of cyclin B in *Aspergillus nidulans*. *J. Cell Biol*. **141**, 1575-1587.